A hybrid BEM-CFD model for effective numerical siting analyses of wind turbines in the urban environment

A hybrid BEM-CFD model for effective numerical siting analyses of wind turbines in the urban environment

F Balduzzi[1], S Bigalli[1], A Bianchini[1]

[1] Department of Industrial Engineering, Università degli Studi di Firenze, Via di Santa Marta 3, 50139, Firenze, Italy.

Corresponding author: bianchini@vega.de.unifi.it

Abstract. The analysis of wind turbine wakes and their interaction with other machines installed in the same array or park has become a key element in the current wind energy research. If in case of siting of large rotors for energy production the use of high-fidelity CFD simulations is well established yet, there is still a lack of knowledge in the analysis of proper wind turbine siting for small wind turbines, which are typically installed in quite complex environments. The present study provides the description and validation of a hybrid BEM-CFD model for the analysis of wind turbine performance and wake structure. With respect to similar existing methods, the proposed one includes a specific correction of turbulence parameters able to make it compatible for use in combination with the standard settings of the turbulence models needed to properly describe the wind profile in the urban environment. The model was then used to carry out a demonstrative sensitivity analysis on the proper siting of a small wind turbine in the rooftop of a typical tall building in a densely built environment.

Nomenclature

A_h	=	Percentage of the total area occupied by buildings (-)
c	=	Turbine blade chord (m)
C_D, C_L, C_p, C_{th}	=	Lift, Drag, Power, Thrust coefficient (-)
C_1, C_2, C_T, C_ε, C_μ	=	Turbulence model constants (-)
C_s	=	Roughness constant (-)
d	=	Displacement (m)
D	=	Distance between UB and IB (m)
f_D, F_D, f_L, F_L	=	Drag, lift force (N)
h	=	UB height (m)
H	=	IB height (m)
$\hat{H}$	=	Mean buildings height (m)
k	=	Turbulent kinetic energy ($m^2\ s^{-2}$)
K_s	=	Sand-grain roughness (m)
Ma	=	Mach number (-)
N_b	=	Number of blades
P	=	Turbine mechanical power (W)
r, R	=	Rotor radius (m)
R^2	=	Coefficient of determination (-)
Re	=	Reynolds number (-)
S_b, S_k, S_ε	=	Source terms for momentum, turbulent kinetic energy, eddy dissipation

TKE	=	Dimensionless turbulent kinetic energy (-)
U	=	Wind speed (m s^{-1})
u^*	=	Friction velocity (m s^{-1})
V_{cell}	=	Mesh cell volume (m^3)
x, y, z	=	Cartesian coordinates (m)
y_p	=	Height of the ground cells centroid (m)
z_0	=	Roughness length (m)
α	=	Incidence angle (rad)
γ	=	Skew angle (deg)
ε	=	Turbulent kinetic energy dissipation rate (m^2 s^{-3})
κ	=	Von Karman constant (-)
μ, μ_T	=	Molecular, turbulent viscosity (kg m^{-1} s^{-1})
ρ	=	Density (kg/m^3)
ABL	=	Atmospheric Boundary Layer
BEM	=	Blade Element Momentum
CFD	=	Computational Fluid Dynamics
HAWT	=	Horizontal-Axis Wind Turbine
IB	=	Installation Building
RANS	=	Reynolds-Averaged Navier-Stokes
TC	=	Turbulence Correction
TSR	=	Tip-Speed Ratio
UB	=	Upwind Building
VBM	=	Virtual Blade Model
WT	=	Wind Tunnel
$_{0, \infty}$	=	Freestream value

1. Introduction and motivation of the study

An effective exploitation of the wind potential in the built environment is becoming a key topic in the present wind energy research on small and medium rotors [1], since the possibility of producing energy exactly where it is needed could make the cost of energy of small turbines more competitive with larger installations. The wind conditions in the rooftop of a building or in its surroundings are however very complex, and generally characterized by high turbulence [2], pulsating flow and misalignment angles with respect to the streamwise direction [3]. The conventional siting aspects of a new turbine then require even more attention than in a conventional site.

If the use of computational fluid dynamics (CFD) is well established for large-scale wind farm simulations, even using high-fidelity approaches like the large-eddy simulation [4], in case of the siting of small machines it is instead not so common to perform dedicated numerical studies for an accurate evaluation of both the local wind conditions and the corresponding energy yield potential. Since the flow conditions above the roof of buildings are different and more complex with respect to an open landscape, the identification of the main characteristics of a suitable site in the built environment is being only addressed in current studies from academia (e.g. [5]). In particular, few examples do exist in the literature concerning the prediction of the actual energy production of a roof-mounted turbine, mainly due to the remarkable complexity and computational cost of the simulation. It has to be noticed that similar approaches require the solution of very different flow length scales, ranging from the large ones related to the urban landscape to the very small ones related to the solution of the flow past airfoils. Considering the low investment costs available for a small turbine installation, the use of a fully resolved approach seems not represent an affordable solution. On this basis, the development of reliable and robust simplified numerical tools for predicting the attended performance in an urban siting could be of major relevance in view of more accurate feasibility analyses. The present study indeed reports a newly-developed adaptation of the Virtual Blade Model (VBM) for ANSYS® FLUENT® for use in the urban environment. In particular, additional sources of turbulence are introduced in the solved flow field to adapt the standard CFD settings typical of the simulation of urban flows to the requirements needed by the VBM model for a correct prediction of

the turbine performance. The use and calibration of the additional sources has been carried out in comparison to a full Reynolds-Averaged Navier-Stokes (RANS) calculation. The same were then used to perform a sensitivity analysis on the most suitable rooftop mounting position of a small horizontal-axis wind turbine (HAWT) in the urban environment.

2. Methodology

2.1. VBM code

The Virtual Blade Model (VBM) is a user-defined function implemented in the commercial solver ANSYS® FLUENT®. It was originally conceived for helicopter aerodynamics but recently it was successfully applied to wind turbine analysis [6]. Some of the authors has already used the VBM to model horizontal-axis wind turbines under conventional inflows [7] and they validated it against experiments in case of single rotor, turbine array or misaligned flow conditions [8]. The VBM was introduced to combine the accuracy of a RANS simulation with a reduced computational cost, since it does not require the explicit discretization of the rotor blades.

In the VBM, the rotor is represented as a disk fluid zone located within the annular area swept by the turbine. The momentum sources represent the effect of the blade forces on the fluid flow and they are introduced in each of the computational cells in the rotor disk region. In the model, the time-averaged aerodynamic effect of the blades is accounted for through a momentum source term placed inside the disk fluid zone, calculated by the Blade Element Momentum theory (BEM), while the rest of the domain is solved using a conventional RANS approach. The rotor is discretized into a finite number of spanwise sections (Figure 1). The blade properties, such as chord length, airfoil type and blade twist angle are allowed to vary along the blade span. First, the velocity field is used to obtain the local angle of attack (α) at each blade element. Using a look-up table with lift and drag coefficient (C_L, C_D) for different angle of attack, Mach number (Ma) and Reynolds number (Re), the instantaneous aerodynamic forces are calculated by Equation 1 on each rotor section:

$$f_L = C_L(\alpha, Ma, \mathrm{Re}) \cdot c(r/R) \cdot \frac{\rho U_{tot}^2}{2} \quad ; \quad f_D = C_D(\alpha, Ma, \mathrm{Re}) \cdot c(r/R) \cdot \frac{\rho U_{tot}^2}{2} \tag{1}$$

where U_{tot} is the relative velocity, c is the chord depending on the blade span and ρ is the fluid density. Assuming a constant rotational speed, the time-averaged lift and drag forces are then calculated with Equation 2:

$$F_{L,cell} = N_b \cdot \frac{dr \cdot d\theta}{2\pi} \cdot f_L \quad ; \quad F_{D,cell} = N_b \cdot \frac{dr \cdot d\theta}{2\pi} \cdot f_D \tag{2}$$

where N_b is the number of blades, r is the spanwise coordinate and θ is the azimuthal coordinate. The source term for the momentum equation of each cell (having a volume V_{cell}) is finally calculated with Equation 3:

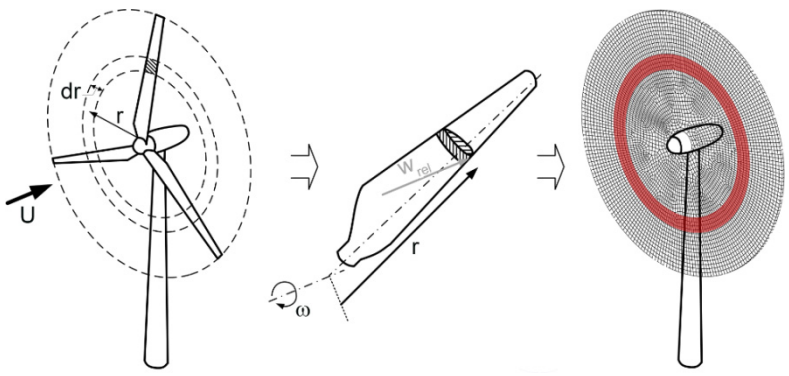

Figure 1. Schematic representation of the equivalence between a rotor blade element and the corresponding VBM annular area.

$$\vec{S}_{b,cell} = -\frac{\vec{F}_{cell}}{V_{cell}} \tag{3}$$

The VBM uses the approximation of a 2D flow during calculation of the local aerodynamic forces. This assumption is violated near the blade tip, where the increased secondary flow results in a reduced lift. Tip loss effects are accounted for by defining a loss proportional to the effective span.

2.2. Turbulence Correction

Some of the authors already pointed out in [7] the inability of such a simplified model to correctly predict the turbulence in the flow. Indeed, the aerodynamic interaction between the blade and the flow is not directly modelled and then the VBM is not able to predict the modification of the turbulent field connected to such interaction. Although this deficiency is deemed not to represent a limiting issue when simulating the turbine in a low turbulence environment (e.g. a wind tunnel or an open landscape), some inaccuracies may arise in case of a high turbulence environment. Therefore, the authors further enhanced the VBM model by introducing additional source terms to the transport equations for the turbulent quantities, according to the original proposal of [9].

The standard k-ε turbulence model is used. The transport equations for k (Equation 4) and ε (Equation 5) are the following:

$$\frac{\partial(\rho k)}{\partial t} + \frac{\partial(\rho k u_i)}{\partial x_i} = \frac{\partial}{\partial x_j}\left[\left(\mu + \frac{\mu_t}{\sigma_k}\right)\frac{\partial k}{\partial x_j}\right] + G_k - \rho\varepsilon + S_k \tag{4}$$

$$\frac{\partial(\rho \varepsilon)}{\partial t} + \frac{\partial(\rho \varepsilon u_i)}{\partial x_i} = \frac{\partial}{\partial x_j}\left[\left(\mu + \frac{\mu_t}{\sigma_\varepsilon}\right)\frac{\partial \varepsilon}{\partial x_j}\right] + C_1\frac{\varepsilon}{k}G_k - C_2\rho\frac{\varepsilon^2}{k} + S_\varepsilon \tag{5}$$

where μ_t is the turbulent viscosity, σ_k and σ_ε are the turbulent Schimdt numbers, C_μ is a typical model constant and G_k is the production of turbulent kinetic energy.

A customized version of VBM model was created by adding additional source terms for the turbulent kinetic energy (S_k) and the eddy dissipation (S_ε) in their transport equation just in front of the rotor [9].

The additional source terms in the transport equations were modelled as in Equation 6:

$$S_k = C_T \cdot \left\| \vec{F} \cdot \vec{U}_\infty \right\| \cdot (1 - C_\varepsilon) \quad ; \quad S_\varepsilon = \frac{\varepsilon}{k} \cdot C_T \cdot \left\| \vec{F} \cdot \vec{U}_\infty \right\| \cdot (C_1 - C_2 \cdot C_\varepsilon) \tag{6}$$

where C_1 and C_2 are the model constants of the k-ε turbulence closure model.

The term C_T is assumed to be a function of the thrust coefficient of the wind turbine: following the recommendation of [9], a direct proportionality is assumed (C_T = 0.24·C_{th}). C_ε is instead a typical parameter of this model and it depends on the wind velocity, the tip speed ratio (TSR) and the blade properties of the wind turbine.

3. Set up

3.1. Study cases for the rooftop siting

A siting analysis for a typical rooftop installation in an urban environment was carried out. Two urban landscape configurations were selected, in order to achieve: a) a suitable compromise between high velocity and moderate skew angles; or b) the maximum accelerating effect regardless of the skew.

In a previous study [10], some of the authors reported the results of a CFD study for the evaluation of the energetic suitability of a small HAWT installation in the rooftop of a building through the use of the VBM model. Since the turbulence sources were not yet implemented, the code was not fully adapted for use in a high-turbulence urban flow. Therefore, the present study reports the results of the newly-developed adaptation of the VBM model for use in the urban environment to verify its potential. One could also argue that a RANS approach is not fully adequate to capture the complex

flow interactions taking place between the oncoming wind, the building and the turbines. Of course, an unsteady approach, or even a higher-fidelity CFD method, could give more accurate results; however, it should be also remembered that the different length scales that need to be solved would imply a tremendous calculation cost, thus making this kind of analyses barely feasible. In this view, the calibration of a simplified RANS approach could find room for a wide diffusion.

The urban landscape configurations were selected according to [10-11], where some of the authors carried out a parametric CFD analysis to characterize the flow field on the rooftop of the installation building (IB) as a function of the geometrical proportions of the surrounding landscape. Figure 2 shows a side view of the computational domain for the urban landscape, where all of the distances of the boundaries were imposed based on the IB height H, as suggested by [12]. The local acceleration on the upwind corner of IB was evaluated for several cases by varying the installation building height, the height h of its upwind building (UB) and the distance D between the buildings themselves. Highest accelerations were observed for an IB height quadruple than the city average height ($\hat{H}$) in case of a close distance between IB and UB. Therefore, in the present analysis, fixed values of H=4$\hat{H}$ and D=0.5$\hat{H}$ were selected for both the analysed landscape configurations.

The two selected environments differ in the UB height only. The compromise between high velocity and low skew angle is obtained when considering h=3.25$\hat{H}$ (*Environment 1*), while the maximum acceleration is obtained when h=2.5$\hat{H}$ (*Environment 2*). Both environments were first simulated without the use of VBM to characterize the flow above the roof of IB in absence of an installed turbine.

A 2 m diameter study HAWT was then designed by means of an aerodynamic scaling of the NREL Phase II [13]. Since the local flow conditions in the area above the roof of the installation building show a large variability, different rotor configurations were investigated (Figure 3). The aim was to show the importance of an optimized positioning of the turbine based on the specific site location in order to exploit the maximum available power as the most convenient practice. To this purpose, three siting strategies were tested:

- *edge*: rotor plane aligned with the building façade, considering a 4 m tower;
- *centered*: rotor with a 4 m tower in the roof center, for stability and aesthetical reasons;
- *optimized*: optimized through the dedicated CFD simulation of the local flow conditions. Four tower heights were tested, since the flow properties strongly depend on the height above the roof.

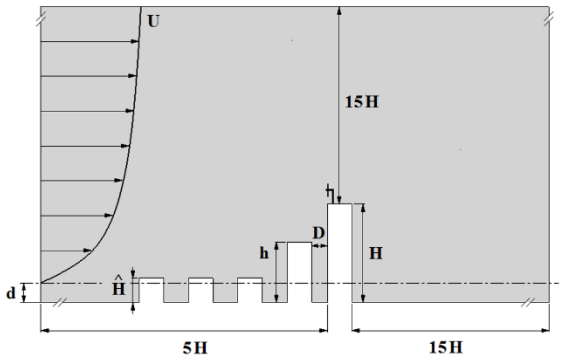

Figure 2. Computational domain [10].

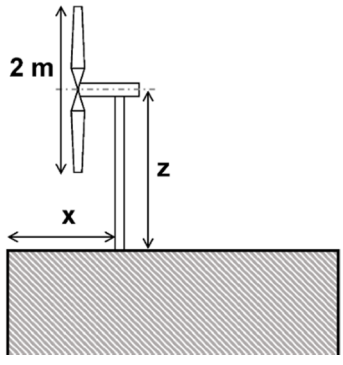

Figure 3. Analysed rotor configurations.

3.2. Computational grid

The dimensions of the computational domain (Figure 2) were imposed as a function of the tallest building in the investigated site (H). The inlet boundary and the domain width were set to 5H, while the outlet boundary and the domain height were set to 15H. When using the VBM model, the CFD domain is divided in two separate fluid regions, i.e. the VBM disk replacing the blades and the region of the external ambient. The two zones are in communication via General Grid Interfaces.

Regarding the discretization of the fluid region of the VBM disk, the mesh sensitivity analysis was carried out on the test case of Andersen [14]. Starting from the maximum refinement level intrinsically allowed by the VBM tool itself (≈ 8000 elements inside the disk), four meshes (labelled from M4 to M1) were defined by progressively halving the number of elements, in order to find the best balancing between accuracy and computational effort. The grid independency was evaluated based on the accuracy in reproducing the wake profiles. To this end, the coefficient of determination (R^2) between the wake profiles at 2*R*, 6*R* and 10*R* downstream the rotor - calculated with reference to the most refined mesh M4 - was evaluated (Figure 4). Mesh independent results were obtained with the third level of refinement (corresponding to roughly ≈ 4000 elements in the VBM region), being R^2>98% for all of the analysed distances.

The mesh of the external ambient was obtained by means of an unstructured tetrahedral grid with a prismatic layers zone in the near-wall regions for capturing the boundary layer. Starting from the mesh sensitivity analysis carried out in a previous 2D study by some of the authors [11], the same level of refinement was used also in the present 3D analysis in terms of sizing of the elements, near-wall discretization and cells expansion ratio. In detail, the study presented in [11] demonstrated for the same environment the need of approximately $1.2 \cdot 10^5$ cells (in 2D). The mesh independency was obtained by progressively reducing the expansion ratio between adjacent cells from the common threshold derived from the literature (1.30) up to the value of 1.08. In addition, a proper refinement in the region surrounding the virtual rotor was also introduced here, in order to accurately solve the flow field on the rooftop. As a result, the grid size was made of roughly $6.5 \cdot 10^6$ cells. It is worth observing that the VBM approach does not require a substantial increase of the mesh size with respect to the case of a simple urban landscape. Indeed, both *Environment 1* and *Environment 2* require roughly $5.1 \cdot 10^6$ cells for the simulation of the atmospheric boundary layer evolution in the urban landscape, i.e. only a 25% reduction with respect to a VBM simulation. Figure 5 reports a view of the mesh for the discretization of the building walls (grey), and a slice of the mesh (light blue) along the vertical mid-plane to show the mesh details in the fluid region. The increased-density zone around the turbine rotor, also comprising a considerable part of the domain downstream the IB, are clearly visible.

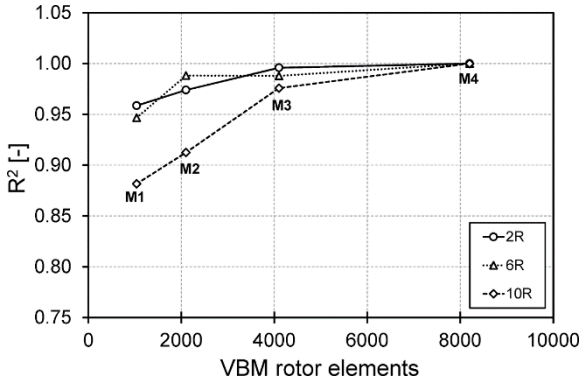

Figure 4. Mesh sensitivity analysis for the VBM.

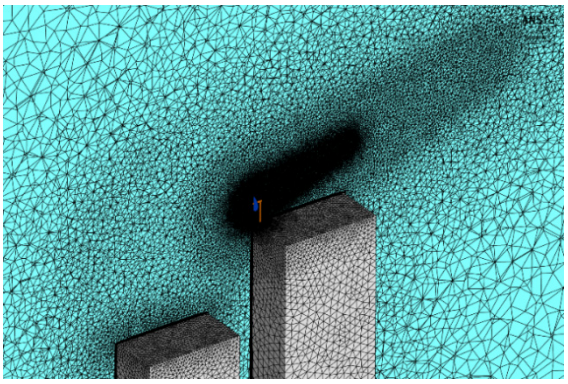

Figure 5. Computational grid for the urban landscape.

3.3. Atmospheric Boundary Layer simulation

In a simulation of the Atmospheric Boundary Layer (ABL) flow in urban locations a correct modelling of the roughness of both the terrain and the city is pivotal. The velocity profile is a log-law profile with a shift of the zero-velocity height (displacement, *d*) depending on the average height of the city buildings (Figure 2). The standard wall functions are used in combination with the equivalent sand-grain roughness K_s to the wall-adjacent cells to express the effect of terrain on the flow. Blocken et al. [15] found a relationship between K_s and the roughness length z_0 (Equation 7):

$$K_s = 9.793 \cdot z_0 / C_s \tag{7}$$

where C_s is a constant varying between 0 and 1. The near-wall cell size is related to the roughness, since the distance from the wall of the first mesh node y_p must satisfy the condition of $y_p > K_s$. For z_0 values in the urban context (~1.0 m), the mesh size at the ground would be excessively large (y_p~30 m) if compared to the grid size on the building walls (z_0=3.0·10^{-4} m, y_p~0.01 m). To overcome this issue, an explicit modelling of the urban roughness was applied through a row of three square blocks (Figure 2) having the function of reproducing the real roughness effect on the flow. By doing so, the z_0 value of an open-landscape surface was used at the ground to reduce the first cell height (z_0=3.0·10^{-2} m). The steady-state three-dimensional simulations were carried out using the commercial code ANSYS® FLUENT®. The Reynolds-averaged Navier–Stokes (RANS) approach was adopted in a pressure-based formulation. Some of the authors have already assessed and validated the main settings for a proper numerical setup for the simulations of the ABL in [11] using the OpenFOAM® open-source code. The setup was validated against experimental wind tunnel measurements of the CEDVAL laboratory [16] on a test case consisting of a single building block (1:200 scale). For the sake of completeness, the main numerical settings are shortly summarized below. The turbulence closure was achieved by means of the *Standard k-ε* model, since its application is recommended in free shear flows as suggested by [5,12]. On the other hand, ε-based models tend to over-estimate the turbulent kinetic energy in the separated region, but an accurate prediction of the flow within this zone is not necessary since the goal is to place the turbine in zones with no recirculation. The pressure-velocity coupling was made with the SIMPLE algorithm and the residuals convergence was set to 10^{-6} for the whole set of RANS equations. The second order upwind scheme was used for the spatial discretization of the equations.

The boundary conditions (Equation 8) were imposed at the domain inlet by the assumption of a constant shear stress with the height, according to the ABL definition [17]:

$$U(z) = \frac{u^*}{\kappa} \ln \frac{(z-d)}{z_0} \quad ; \quad \varepsilon(z) = \frac{u^{*3}}{\kappa z} \quad ; \quad k(z) = \frac{u^{*2}}{\sqrt{C_\mu}} \tag{8}$$

where u^* is the friction velocity and κ is the von Karman constant. The roughness properties and the wind characteristics were specified based on a real city data set. In particular, literature data for London city [18] were chosen (Table 1). The displacement value d was calculated by Equation 9, following the indications of the ESDU [19]:

$$d = \hat{H} - 4.3 z_0 \left(1 - A_h\right) = 13m \tag{9}$$

Table 1. Roughness properties and wind characteristics (London data).

$\hat{H}$	A_h	z_0	u^*
13.6 m	55%	0.29 m	0.55 m/s

4. Results

4.1. Wind tunnel validation

As discussed, the VBM code with Turbulence Correction (VBM-TC), i.e. with additional source terms for turbulent kinetic energy and its rate of dissipation, is used. The original model was previously validated with the wind tunnel test case of the NREL Phase VI rotor in low turbulence conditions [7]. Some of the authors performed a full CFD RANS simulation of the rotor blades obtaining good matching with the experimental results in terms of torque characteristic curve and pressure coefficient distributions on the blade surface. The flow filed solution of the full rotor was then used as a benchmark for the validation of the VBM module in terms of wake analysis and turbine performance.

The same test case was here used for validating the newly modified version of the VBM model and to evaluate the improved prediction capability in case of a high turbulence environment. In order to carry out a comparison with the RANS approach, the same computational grid was used. Figure 6 and Figure 7 show the mesh details and the computational domain of the RANS simulations, respectively.

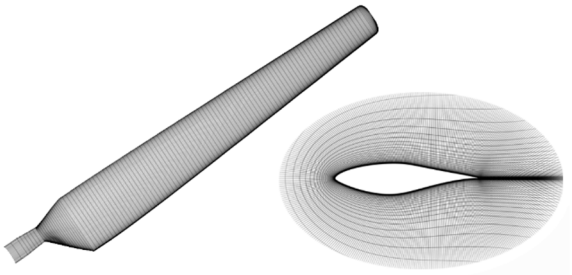

Figure 6. Details of the computational mesh [7].

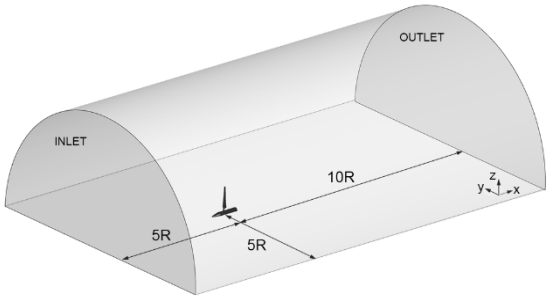

Figure 7. Full rotor 3D computational domain [7].

To impose a suitable turbulence level, the inlet boundary conditions for k and ε were defined by considering the same turbulence level experienced by the turbine in the urban context. Therefore, the inlet turbulent quantities were computed with Equations 8 at the elevation of IB.

The outcome of the validation study is plotted in Figure 8, where the results obtained with the VBM-TC code are compared with the full RANS and original VBM results.

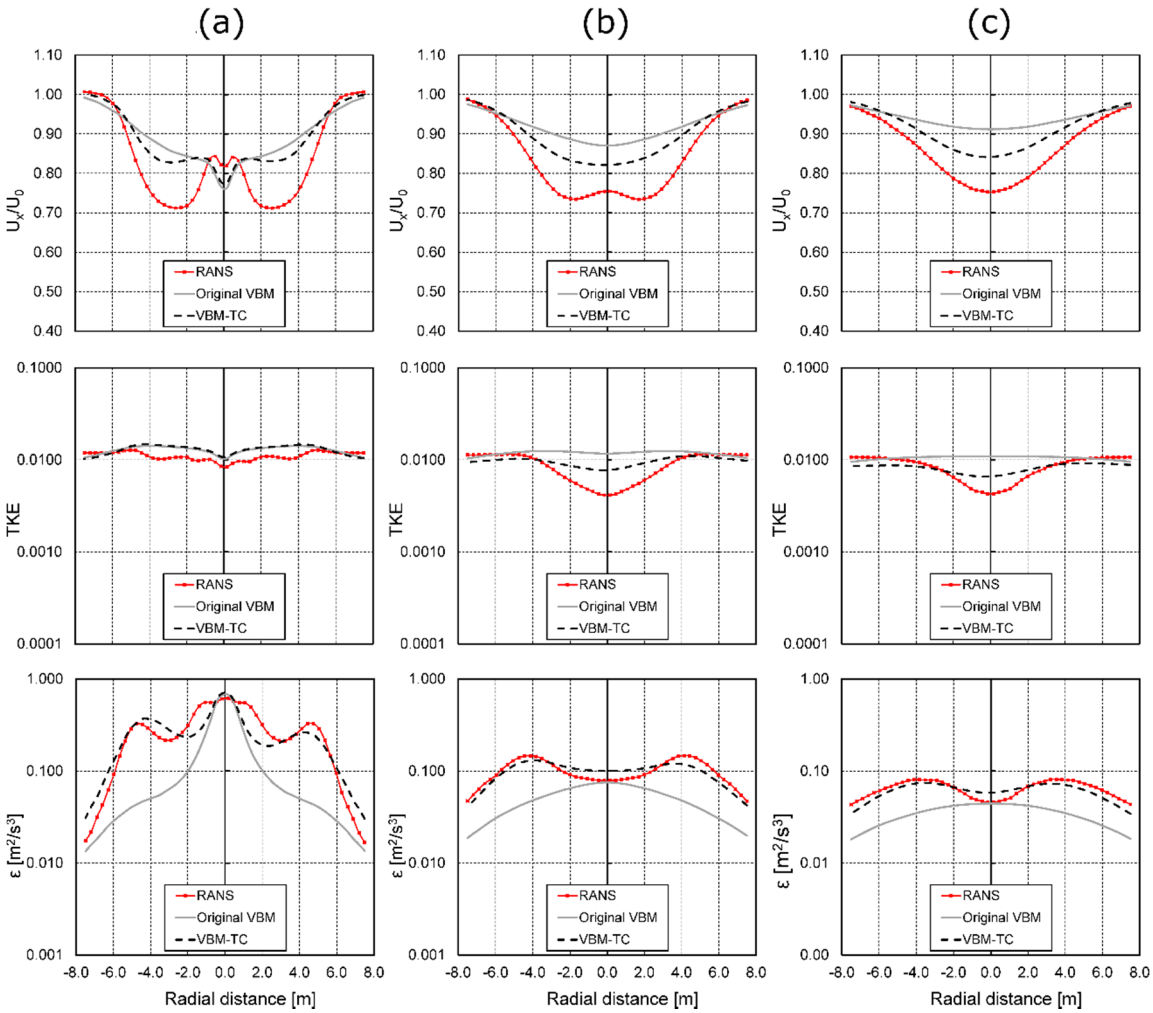

Figure 8. Profiles of velocity deficit, *TKE* and ε in the rotor wake with the three investigated models at different distances from the rotor: (a) 2*R*; (b) 6*R*; (c) 10*R*.

The wake evolution is evaluated in terms of velocity deficit (U_x/U_0), dimensionless turbulent kinetic energy ($TKE \equiv k/U_0^2$) and turbulent dissipation rate at three distances downstream the rotor (Near Wake - 2*R*, Mid Wake - 6*R*, Far Wake - 10*R*). Assuming the RANS results as the benchmark (since the use of the RANS approach is expected for the simulation within the urban environment), it is apparent that the additional source terms in the corrected model are able to strongly improve the prediction of the turbulent quantities in the rotor wake. In particular, the ε profiles at all of the three distances match almost exactly with the full rotor solution, as well as the *TKE* values in the region away from the rotor show a better agreement.

As a result, the prediction of the velocity deficit is also enhanced. Indeed, the original VBM showed a large overestimation of the velocity at all distances in the rotor wake, while the VBM-TC model is able to capture the wake shape. The addition of calibrated source terms in the transport equations of k and ε is therefore necessary to improve the prediction of the wake shape in case of an incoming flow with high turbulence. As a final remark, it is worth pointing out that the VBM-TC code was also tested in case of a standard wind tunnel turbulence level, showing a negligible influence on both the velocity and the turbulent quantities.

4.2. Wall effect in the built environment

A characterization of the flow above the roof of IB was first performed to identify the presence of locally accelerated flow for the maximization of the energy extraction. To this purpose, CFD simulations of the urban environment were first performed without the turbine to investigate the flow field modifications on the rooftop of IB when different heights of UB are considered. Figure 9 reports the contours of the velocity component along the rotor axis (U_x) on the central vertical plane for both *Environment 1* and *Environment 2*. The values are reported in a dimensionless form with respect to the undisturbed velocity at the same height (Equation 8) to clearly highlight the acceleration and deceleration areas for the correct choice of the best position.

The wall effect of the oncoming flow can be clearly observed, since high-rise buildings strongly interact with the incoming wind, leading to regions of accelerated flow. The *edge*, *centered* and *optimized* positions on the rooftop where the turbine is thought to be installed are also represented. It is apparent that neither the *edge* nor the *centered* rotor configurations are located in the zone of maximum acceleration. Moreover, the location of the U_x peak depends on the height of UB and the separation zone has a larger extension for *Environment 2*, due to a different interaction with a lower building. The values of both the velocity modulus and the skew angle of the flow approaching the turbine are shown in Figure 10 and Figure 11, respectively, for the two environments and the three different rotor positions.

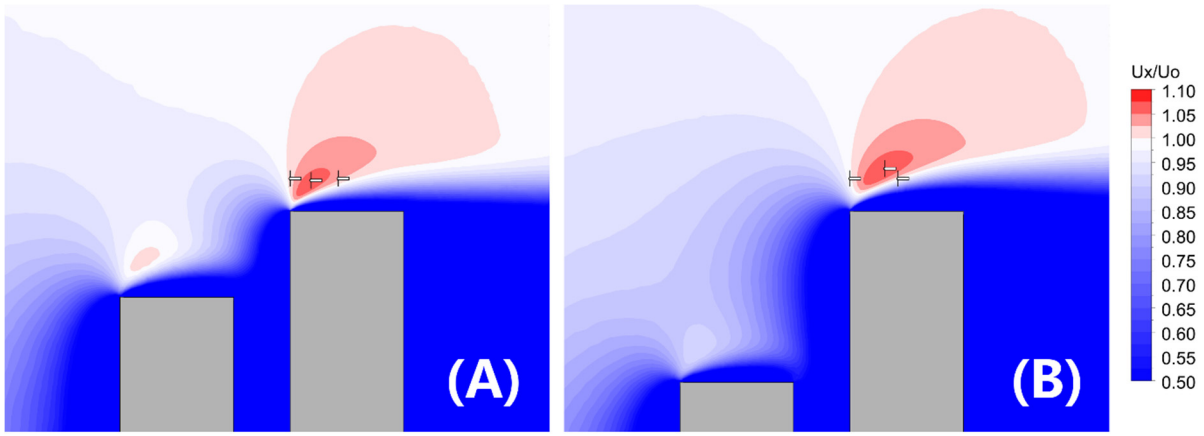

Figure 9. Dimensionless *x*-velocity contours: A) *Environment 1*; B) *Environment 2*.

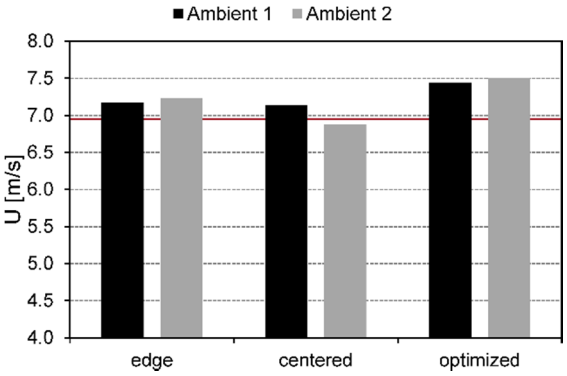

Figure 10. Results for the two environments depending on the rotor position: velocity magnitude.

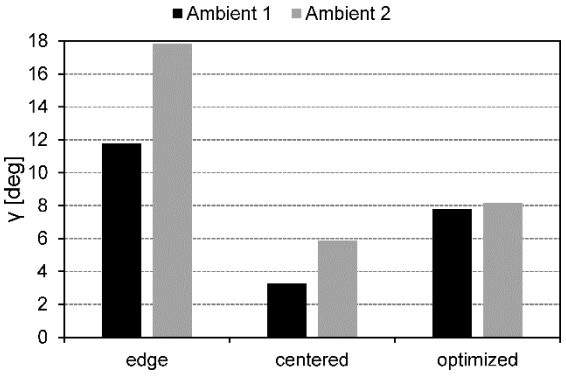

Figure 11. Results for the two environments depending on the rotor position: skew angle.

The values are averaged over the area "potentially" occupied by the rotor. The positions aligned with the building façade suffer from high skew angles of the flow, while the centered positions are characterized by a straightened flow, even if the wind speed is the lowest among the considered positions. For both environments, the optimal configurations represent the trade-off between high velocity and moderate skew angles, with a slight higher acceleration in case of a lower UB height.

4.3. Turbine performance

In order to have a benchmark for the simulations using the VBM in the built environment, a preliminary analysis was carried out in wind tunnel-like conditions to evaluate the performance of the turbine in aligned flow [10]. The power coefficient (C_p) curve of the rotor was calculated within a cylindrical domain by varying the rotor revolution speed with a constant inflow velocity of 6.95 m/s, corresponding to the velocity value at the installation height in undisturbed condition (according to Equations 8). A maximum C_p of 0.355 was obtained at TSR=6.

The VBM-TC was then used to simulate the performance of the wind turbine in both *Environment 1* and *Environment 2*. Due to the small difference between the undisturbed velocity and the local values of velocity in the installation site (Figure 10), as already discussed the TSR=6 condition reasonably represented the power peak for all of the tested configurations. Accordingly, the rotational speed of the wind turbine was varied as a function of the variation of the local U_x. The power extracted by the rotor was calculated with the improved VBM for all of the simulated cases and compared with the wind tunnel case. The results were also post-processed in terms of C_p by considering the values of local velocity evaluated in the simulations of the urban landscape (U_{local}). Moreover, the power output was compared with the theoretical power (P_{th}), i.e. the power calculated using the C_p value of the wind tunnel and the velocity at each installation position U_{local} of the wind turbine using Equation 10:

$$P_{th} = C_{p,WT} \cdot \left(\frac{1}{2} \rho \pi R^2 U_{local}^3 \right) \tag{10}$$

The results for both *Environment 1* and *Environment 2* are shown in Figure 12 and Figure 13 respectively. In both urban landscapes the maximum power occurs in the *optimized* configurations, in agreement with the expectations derived from the analysis of Section 4.2. It is worth noticing that the power extracted by the VBM is always lower than expectations. Indeed, although the rotor would be supposed to work in conditions of accelerated flow with respect to the undisturbed wind at almost every position (according to Figure 9), only the *optimized* configuration in *Environment 1* is able to provide a slightly higher power. The reason of this discrepancy is related to the fact that P_{th} is calculated with the hypothesis of a uniform inflow profile, while the actual working condition is characterized by the presence of large velocity gradients and by the interaction of the rotor wake with the separated region above the building roof.

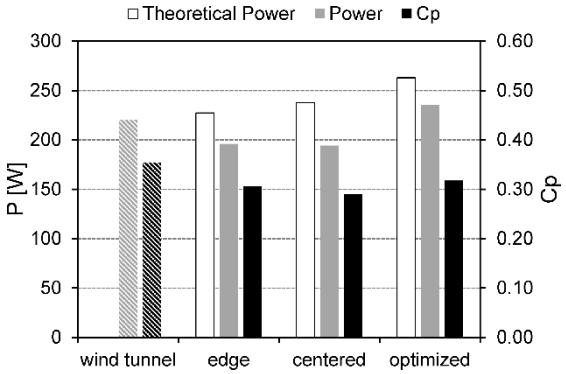

Figure 12. VBM results in *Environment 1*.

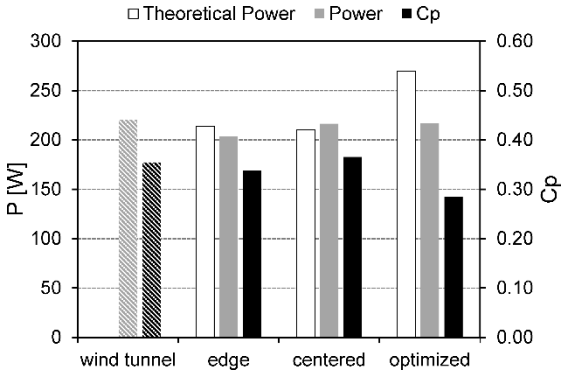

Figure 13. VBM results in *Environment 2*.

As a result, the values of C_p are lower than the wind tunnel benchmark, down to 0.285 for the *optimized* configuration in *Environment 2*. The *centered* configuration in *Environment 2* is the only exception, since the power extracted is higher than theoretical one, leading to a C_p of 0.365. These results testify that the efficiency is strongly dependent on the specific position when placing the machine in a non-uniform flow. Therefore, if the position is not properly optimized, the turbine is not able to exploit the whole potential derived from the acceleration on the rooftop of IB and the theoretical computation of the expected power may result in misleading results.

Since the largest variability of the results was observed for *Environment 2*, Figure 14 reports the dimensionless axial velocity contours for the three different positions of the turbine (see Figure 9.b).

From a perusal of the figure, it can be observed that the wind turbine in the *optimized* case (Figure 14.c) is not able to suitably harvest the available energy since the peak of axial velocity directly impacts on the hub region, without producing power. Conversely, the accelerated flow directly impacts the blades in the upper half of the rotor in the *centered* case (Figure 14.b), with a more effective energy extraction. Finally, in the *edge* case (Figure 14.a) the rotor operates in a region outside the acceleration zone above the roof, corresponding to a more uniform inflow condition. Therefore, the power output is more similar to what expected from the wind tunnel results. As a result, the power coefficient for the *optimized* case is the lowest, despite the value of axial velocity at the turbine inlet is maximum. It is worth remembering that the velocity values computed with the simulations for the urban landscape are averaged over the area occupied by the rotor.

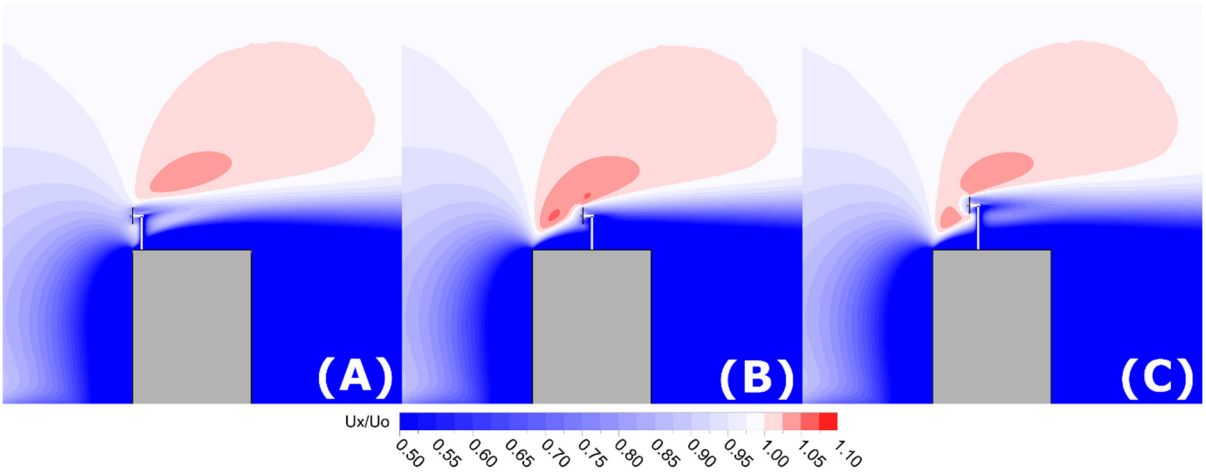

Figure 14. Dimensionless *x*-velocity contours in *Environment 2* for configurations: A) *edge*; B) *centered*; C) *optimized*.

Therefore, to investigate the possibility of better exploiting such a region of high velocity flow, an additional sensitivity analysis on the tower height was carried out. Maintaining the wind turbine in the *optimized* position, three further simulations were performed by varying the height of the VBM disk with respect to the *baseline* of Figure 14.c. In detail, the positions -1*D*, -0.5*D* and +0.5*D* were tested.

Figure 15 reports the power output for all of the considered rotor heights, expressed in a dimensionless form with respect to the power of the *baseline* case. The power increases when the rotor is in a lower position, with a maximum of +23% for the configuration at -0.5*D*. The power extraction is maximized, since the value of expected power reported in Figure 13 is reached. The corresponding C_p is now 0.358, hence the turbine is extracting energy in a more effective way. Indeed, the turbine is now working in a condition more similar to Figure 14.b, i.e. the accelerated flow directly impacts the central portion of the blades instead of the hub region.

5. Conclusions

The study presents the introduction of specific turbulence source terms in the flow field to adapt the Virtual Blade Model for ANSYS® FLUENT® for use in siting analyses in the urban environment. In further detail, the proposed modifications allow the user to adapt the standard CFD settings typical of urban flows to the requirements needed by the VBM model for a correct turbine simulation. A comparison with a full RANS calculation proved the effectiveness of the approach. The new model was then exploited to perform a sensitivity analysis about the rooftop siting of a small HAWT, demonstrating the prospects of using numerical simulations for similar analyses. Two urban landscape configurations were selected, in order to achieve respectively: a) a suitable compromise between high velocity and moderate skew angles; b) the maximum accelerating effect regardless of the skew. Three different mounting locations of the turbine were investigated. The results showed that:

- the flow conditions on the IB roof are strongly variable, thus requiring dedicated CFD simulations;
- if the rotor position is properly optimized, a large power increase can be obtained with respect to a "reasonable" positioning based on generic considerations;
- the simulation of the urban landscape only is not sufficient to accurately assess the best rotor positioning and the expected power due to the presence of strong velocity gradients, which lead to a large variation of the working condition of different portions of the blade;
- in the present case study, the VBM-TC model showed that a positioning of the rotor 0.5*D* below the location of maximum *x*-component of velocity can lead to a 20% increase of the output power;
- due to the non-uniformity of the velocity distribution, a strong influence of the selected site on the C_p was observed, which can be even higher than the maximum values obtained in a wind tunnel.

Overall, it is mandatory to account for the mutual interaction between the turbine and the rooftop flow for an accurate prediction of the rotor performance and the resulting energy yield. A segregated approach based on the estimated velocity on the rooftop of IB, by means of a theoretical computation of the expected power without a direct simulation of the turbine, in fact may result in misleading results.

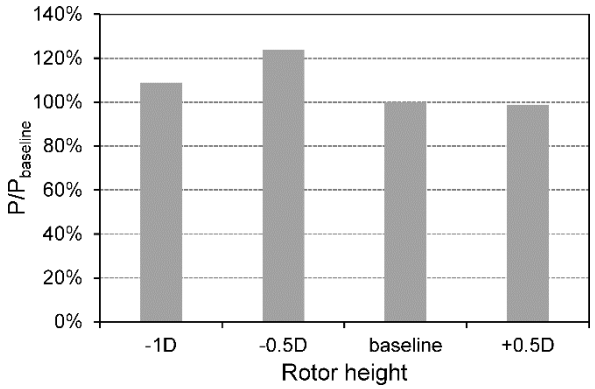

Figure 15. Extracted power as a function of the rotor height for the *optimized* case in *Environment 2*.

Acknowledgments
The activity presented in the paper is part of the research grant assigned to Dr. Francesco Balduzzi by the *Fondazione Cassa di Risparmio di Firenze*, which is sincerely acknowledged for its invaluable effort is sustaining the university research.

References
[1] Barlow JF, Drew DR 2015 Wind flow in the urban environment. WINERCOST Work-shop *Trends and Challenges for Wind Energy Harvesting* (Coimbra, Portugal)
[2] Dallman AR 2013 *Flow and turbulence in urban areas* PhD thesis - Univ. of Notre Dame (USA)
[3] Bianchi S, Bianchini A, Ferrara G, Ferrari L 2013 Small Wind Turbines in the Built Environment: Influence of Flow Inclination on the Potential Energy Yield *J Turbomach* **136**(4) 041013-8
[4] Chivaee HS, Pierella F, Mikkelsen RF, Sørensen JN 2014 Comparison of two LES codes for wind turbine wake studies *Journal of Physics: Conference Series (Online)* **524**(1) 012145
[5] Abohela I, Hamza N, Dudek S 2013 Effect of roof shape, wind direction, building height and urban configuration on the energy yield and positioning of roof mounted wind turbines *Renewable Energy* **50** 1106-1118
[6] Javaherchi Mozafari AT 2010 *Numerical Modeling of Tidal Turbines: Methodology Development and Potential Physical Environmental Effects* MSc Thesis - University of Washington
[7] Bianchini A, Balduzzi F, Gentiluomo D, Ferrara G, Ferrari L 2017 Comparative Analysis of Different Numerical Techniques to Analyze the Wake of a Wind Turbine *Proc. of the ASME Turbo Expo 2017* (Charlotte, USA)
[8] Bianchini A, Balduzzi F, Gentiluomo D, Ferrara G, Ferrari L 2017 Potential of the Virtual Blade Model in the analysis of wind turbine wakes using wind tunnel blind tests *Energy Procedia* **126**(September 2017) 573-580
[9] Hallanger A, Sand IO 2013 CFD Wake Modelling with a BEM Wind Tutbine sub-model *Modeling, Identication and Control* **34**(1) 19-33
[10] Balduzzi F, Bianchini A, Gentiluomo D, Ferrara G, Ferrari L 2017 Rooftop siting of a small wind turbine using a hybrid BEM-CFD model *Wind Energy Exploitation in Urban Environment. TUrbWind 2017 Colloquium* (Springer)
[11] Balduzzi F, Bianchini A, Ferrari L 2012 Microeolic turbines in the built environment: Influence of the installation site on the potential energy yield *Renewable Energy* **45** 163-174
[12] Franke J, Hellsten A, Schlünzen H, Carissimo B 2007 Best practice guideline for the CFD simulation of flows in the urban environment *COST Office* (Brussels)
[13] Mertens S 2003 *The energy yield of roof mounted wind turbines* Wind Engineering **27** 507-517
[14] Andersen B 2013 *Wake behind a wind turbine operating in yaw* MSc thesis - NTNU (Norway)
[15] Blocken B, Stathopoulos T, Carmeliet J 2007 CFD simulation of the atmospheric boundary layer: wall function problems *Atmospheric Environment* **41**(2) 238-252
[16] Leitl B, Shatzmann M 1998 *Compilation of experimental data for validation of microscale dispersion model* CEDVAL Meteorological Institute - Hamburg University
[17] Richards PJ, Hoxey RP 1993 Appropriate boundary conditions for computational wind engineering models using the k-ε turbulence model *J. of Wind Eng. and Ind. Aerodyn.* **46**
[18] Ratti C, Di Sabatino S, Caton F, Britter R, Brown M 2002 Analysis of 3-D urban databases with respect to pollution dispersion for a number of European and American cities *Water, Air and Soil Pollution* **2** 459-469
[19] Engineering Science Data Unit 1984 Strong winds in the atmospheric boundary layer, Part 1: mean-hourly wind speeds *ESDU 82026 with Amendment A and B* London